JACS
JOURNAL OF THE AMERICAN CHEMICAL SOCIETY

Communication

pubs.acs.org/JACS

Electroreduction of Carbon Dioxide to Hydrocarbons Using Bimetallic Cu–Pd Catalysts with Different Mixing Patterns

Sichao Ma,[†,‡,⊥] Masaaki Sadakiyo,[‡,§] Minako Heima,[‡,§] Raymond Luo,[†] Richard T. Haasch,[∥] Jake I. Gold,[†] Miho Yamauchi,[*,‡,§] and Paul J. A. Kenis[*,†,‡]

[†]Dept. of Chemistry and Chemical and Biomolecular Engineering, UIUC, 600 S. Mathews Ave., Urbana, Illinois 61801, United States

[‡]International Institute for Carbon-Neutral Energy Research (WPI-I2CNER), Kyushu University, 744 Moto-oka, Nishi-ku, Fukuoka 819-0395, Japan

[§]CREST, JST, 4-1-8 Honcho, Kawaguchi, Saitama 332-0012, Japan

[∥]Frederick Seitz Materials Research Laboratory, UIUC, 104 S. Goodwin Ave., Urbana, Illinois 61801, United States

Supporting Information

ABSTRACT: Electrochemical conversion of CO_2 holds promise for utilization of CO_2 as a carbon feedstock and for storage of intermittent renewable energy. Presently Cu is the only metallic electrocatalyst known to reduce CO_2 to appreciable amounts of hydrocarbons, but often a wide range of products such as CO, $HCOO^-$, and H_2 are formed as well. Better catalysts that exhibit high activity and especially high selectivity for specific products are needed. Here a range of bimetallic Cu–Pd catalysts with ordered, disordered, and phase-separated atomic arrangements (Cu_{at}:Pd_{at} = 1:1), as well as two additional disordered arrangements (Cu3Pd and CuPd3 with Cu_{at}:Pd_{at} = 3:1 and 1:3), are studied to determine key factors needed to achieve high selectivity for C1 or C2 chemicals in CO_2 reduction. When compared with the disordered and phase-separated CuPd catalysts, the ordered CuPd catalyst exhibits the highest selectivity for C1 products (>80%). The phase-separated CuPd and Cu3Pd achieve higher selectivity (>60%) for C2 chemicals than CuPd3 and ordered CuPd, which suggests that the probability of dimerization of C1 intermediates is higher on surfaces with neighboring Cu atoms. Based on surface valence band spectra, geometric effects rather than electronic effects seem to be key in determining the selectivity of bimetallic Cu–Pd catalysts. These results imply that selectivities to different products can be tuned by geometric arrangements. This insight may benefit the design of catalytic surfaces that further improve activity and selectivity for CO_2 reduction.

Atmospheric CO_2 levels recently have reached 400 ppm and are expected to continue to rise. This increase in CO_2 levels has been associated with undesirable climate effects such as global warming, rising sea levels, and more erratic weather patterns. A variety of strategies (e.g., switching to renewable energy sources, enhancing the energy efficiency of buildings and cars, and capturing carbon from point sources) needs to be pursued to reduce CO_2 emissions and, thereby, curb the increase in atmospheric CO_2 levels.[1] Another promising strategy to help address the issue of high atmospheric CO_2 levels is the electrochemical reduction of CO_2 to useful intermediates or fuels such as formic acid, carbon monoxide, hydrocarbons, and alcohols.[2−5] This process can be driven by the vast amounts of intermittent excess electricity that are becoming available with the rapid increase in the number of solar and wind power plants.

Although the electroreduction of CO_2 to value-added products has promise, the high overpotential of this reaction and low activity of the currently known catalysts still hamper this process from becoming close to commercialization. Cu is the only catalyst known to electrochemically convert CO_2 to hydrocarbons and/or oxygenates at considerably high Faradaic efficiency (FE), but it also produces other products such as CO, $HCOO^-$, and H_2 at fairly high FEs.[6] Intensive research efforts, both experimental (nanostructured Cu catalyst,[7] oxide-derived Cu catalyst,[8−10] etc.) and theoretical (key intermediates,[11] different reaction pathways,[12,13] etc.), have focused on improving the overpotential and selectivity of Cu catalysts for the electroreduction of CO_2 to a specific product. However, the observed Faradaic efficiencies for both C1 and C2 chemicals are typically below 40%. Norskov et al. suggested developing bimetallic Cu-based catalysts to break the scaling relationship and stabilize the reaction intermediate to lower the overpotential.[14] Recently, experimentalists have started to develop various Cu-based bimetallic catalysts such as Au–Cu nanoparticles,[15] polymer-supported CuPd nanoalloys,[16] and Au@Cu core@shell nanoparticles[17] for CO_2 reduction. However, most of these studies only focused on improving the selectivities for C1 products. Also, these reports only studied the effect of composition (ratio of two metals). To date the lack of bimetallic catalysts with well-defined arrangement of respective metal atoms has prevented study of the effect of structure (different mixing patterns of two elements) on product distribution. Here, we pursue a major challenge, the synthesis and characterization of bimetallic catalysts with well-defined elemental arrangements, specifically bimetallic Cu–Pd catalysts with different elemental arrangements (ordered, disordered, phase-separated, Figure 1a) and different atomic ratios (1:3 to 3:1) to study the effect of structure and composition on catalyst activity and selectivity for CO_2 reduction. Possible active sites for the production of C2

Received: October 13, 2016
Published: December 13, 2016

DOI: 10.1021/jacs.6b10740
J. Am. Chem. Soc. 2017, 139, 47−50

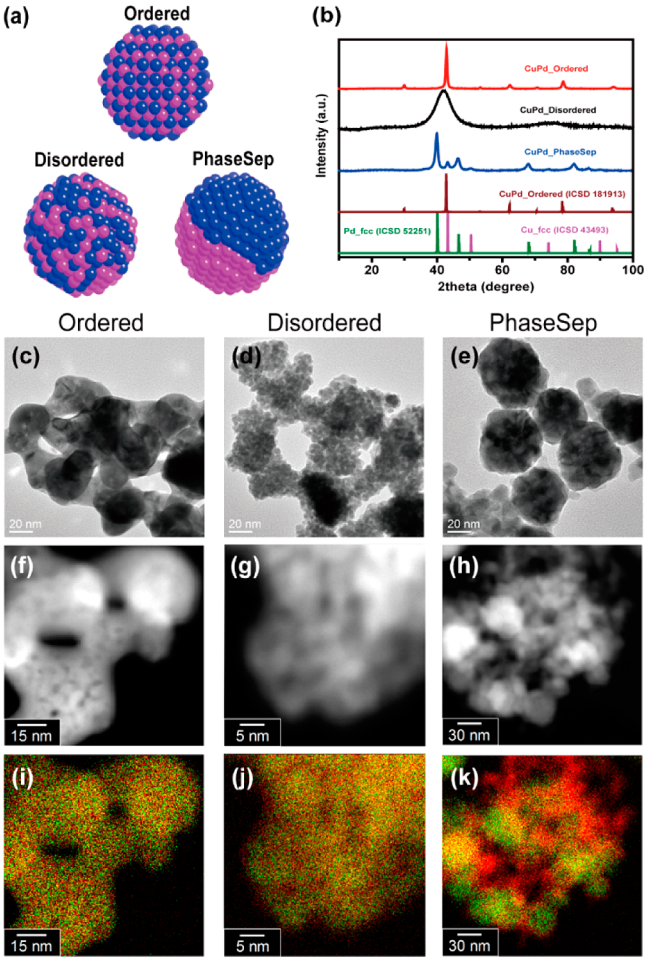

Figure 1. Physical characterization of bimetallic Cu−Pd catalysts with different atomic mixing patterns: ordered, disordered, and phase-separated. (a) Illustration of prepared CuPd nanoalloys with different structures; (b) XRD patterns of prepared CuPd nanoalloys as well as previously reported Cu, Pd and CuPd alloys; (c, d, e) High-resolution TEM images; (f, g, h) HAADF-STEM images; (i, j, k) Combined EDS elemental maps of Cu (red) and Pd (green).

chemicals and CH_4 are proposed based on the electrochemical analysis of the performance of these bimetallic catalysts.

The preparation of the samples studied, a solid-solution type CuPd alloy (disordered sample, Cu_{at}:Pd_{at} = 1:1), an ordered CuPd alloy (Cu_{at}:Pd_{at} = 1:1), a phase-separated (PhaseSep) CuPd sample (Cu_{at}:Pd_{at} = 1:1), as well as a Cu3Pd sample (Cu_{at}:Pd_{at} = 3:1) and a CuPd3 sample (Cu_{at}:Pd_{at} = 1:3), is described in the Supporting Information (SI). The composition of these samples was examined using a scanning electron microscope equipped with energy dispersive X-ray spectroscopy (SEM-EDS). The measured atomic ratios of the various synthesized CuPd samples are summarized in Table S1.

The X-ray diffraction (XRD) pattern (Figure 1b) indicate that the ordered and disordered bimetallic Cu−Pd samples form homogeneous structures. The XRD pattern of the ordered CuPd sample fits well with an ordered B2 structure (Figure S1a) in which alternatively arranged Cu and Pd atoms reside on neighboring sites in a bcc-based lattice, as previously reported.[18] The disordered CuPd sample shows a broad single peak around $2\theta = 42°$, which is likely due to a diffraction from the (011) plane in a bcc-based structure. However, the peaks at higher angles do not match a bcc structure (Figure S1b), implying low crystallinity. The absence of the characteristic peak of the ordered B2 structure around $2\theta = 30°$ ((001) plane) suggests that the Cu and Pd atoms form a disordered structure in this sample. XRD data also reveal that the sample we will refer to as phase-separated is composed of three separate phases: fcc-type Cu, Cu_2O, and fcc-type Pd (Figure S1c).

High-resolution transmission electron microscope (HR-TEM) measurements showed that three CuPd alloys indeed have different morphologies and particle sizes (Figure 1c−e): the ordered sample consists of interconnected crystalline features with a particle size of ∼50 nm; the disordered sample consists of uniform spheres with a particle size of ∼5 nm; the phase-separated sample consists of two aggregates with distinct morphologies: (1) spherical particles ∼50 nm in size and (2) an interconnected structure with smaller particles ∼20 nm in size.

We also examined the chemical microstructure of these three different CuPd alloys using a scanning transmission electron microscope combined with EDS (STEM-EDS) to yield high-angle annular dark-field STEM (HAADF-STEM) images and STEM-EDS maps of the alloys (Figure 1f−k). Similar morphologies as shown in the HR-TEM images were evident from the HAADF-STEM images; however, clear differences in the elemental distributions were observed. The EDS mapping of the ordered sample (Figure 1i) shows that Cu (red) and Pd (green) atoms are homogeneously distributed, forming an ordered intermetallic structure. We could not find large domains composed of only Cu or Pd throughout the disordered alloy particles (Figure 1j). XRD data indicate that this sample has a solid-solution type alloy structure that contains small domains of Cu atoms due to its disordered character (Figure 1a). In contrast, the EDS mapping of the phase-separated sample exhibits separate phases of Cu and Pd elements; within each phase, most of the neighboring sites are from the same element (Figure 1k). In summary, these STEM-EDS results are in good agreement with the XRD results; we successfully obtained ordered, disordered, and phase-separated mixing patterns in the samples.

X-ray photoemission spectroscopy (XPS) results combined with Auger spectra (Figure S2) show that different valence states of Cu exist on the surface of the different bimetallic Cu−Pd samples due to the differences in their elemental arrangement. Note, however, that the initial amount of Cu oxides on the surface does not affect the product distribution significantly in the electroreduction of CO_2, as previously reported.[19]

To evaluate activities of catalysts for CO_2 reduction, each bimetallic Cu−Pd catalyst was deposited onto a gas diffusion layer to form a gas diffusion electrode (GDE), which was assembled in a flow reactor that we reported previously.[19] The electrolysis was performed in a 1 M KOH electrolyte in potentiostatic mode under ambient conditions. Gas- and liquid-phase products were analyzed by gas chromatography (GC) and nuclear magnetic resonance (NMR) spectroscopy, respectively. Figure S3 shows the single electrode polarization curves of the ordered, disordered, and phase-separated samples with Table S2 summarizing total current densities (CDs) using different samples under various potentials. The phase-separated sample achieves the highest total CD of 370 mA cm^{-2}, while the ordered sample has the lowest total CD, indicating that the phase-separated sample exhibits the highest overall production rate among these three samples.

Figure 2a−2d show Faradaic efficiencies (FEs) as a function of cathode potential for each of the major products using the ordered, disordered, and phase-separated CuPd samples. At cathode potentials more positive than −0.3 V_{RHE}, the CO FE is

DOI: 10.1021/jacs.6b10740
J. Am. Chem. Soc. 2017, 139, 47−50

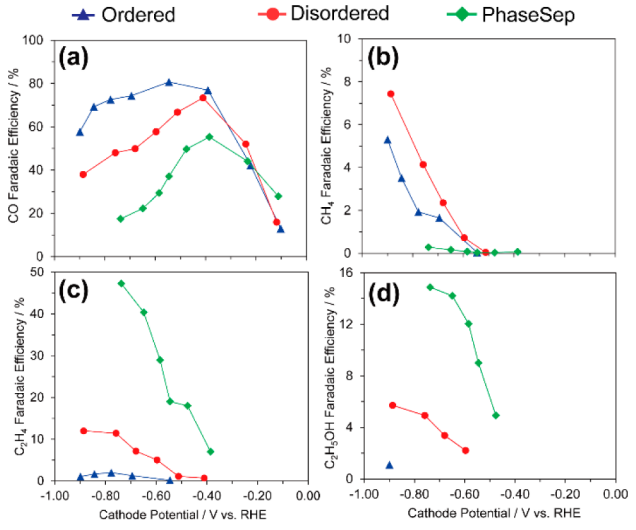

Figure 2. Faradaic efficiencies for (a) CO; (b) CH_4; (c) C_2H_4; (d) C_2H_5OH for bimetallic Cu−Pd catalysts with different mixing patterns: ordered, disordered, and phase-separated.

almost the same for all three samples; at cathode potentials more negative than −0.3 V_{RHE}, where C2 chemicals start to be produced, the ordered CuPd exhibits the highest CO FE, and the phase-separated CuPd achieves the lowest CO FE (Figure 2a). However, for C2 chemicals, the phase-separated CuPd exhibits the highest FE (up to 63%, among the highest reported values for C2 production[19]), and the ordered CuPd has the lowest C2 FE (<5%, Figure 2c and 2d). Note that the FE for ethanol on the phase-separated sample is relatively high, similar to our previous work that reports high FEs for ethanol and ethylene on Cu nanoparticles, indicating that the reaction mechanism for the phase-separated sample is similar to the reaction mechanism on Cu nanoparticles reported previously.[19] The disordered CuPd has a higher FE for CH_4 compared to the FEs observed for ordered or phase-separated CuPd alloys (Figure 2b). This result is in agreement with prior experimental[16] and theoretical studies[14] reporting that alloying Cu with an element with a high oxygen affinity improves the FE for CH_4. Although the ordered CuPd has more alternating Cu−Pd sites than the disordered CuPd, the higher CH_4 FE observed for the disordered sample may be due to a higher surface coverage of the intermediate. All the above observations indicate that (1) CO is an important precursor for C2 chemicals production[12,20] and (2) the phase-separated CuPd catalyst converts adsorbed CO to C2 chemicals more easily than the ordered CuPd catalyst, with the latter converting adsorbed CO more easily to CH_4 than the phase-separated catalyst.

Linking mixing patterns of the catalysts with the trend in FE for C2 products, we suspect that the catalyst structure with dominant neighboring Cu atoms (the phase-separated sample) may favor conversion of CO_2 to C2 chemicals, while the structure with intermetallic mixing patterns (the ordered sample in this study) favors conversion of CO_2 to CH_4. Specifically, in the phase-separated structure, due to the neighboring feature of Cu atoms which may allow for the favorable molecular distance and small steric hindrance, adjacently adsorbed CO will be dimerized easily to the COCOH intermediate. The COCOH intermediate will then be converted mainly to C2 products, with only a small portion decomposing and converting to CH_4. While in the ordered structure, Cu−Pd intermetallic structures are majorly present. The adsorbed CO on a Cu atom tends to form the CHO intermediate with the oxygen atom partially adsorbed on the Pd atom, which stabilizes the adsorption of the CHO intermediate and favors the further production of CH_4, as predicted from prior theoretical studies.[14] Therefore, the dimerization of adsorbed CO, a key step for the production of C2 chemicals, may be preferred on sites with neighboring Cu atoms. Our observations also indicate that the formation of CH_4 and C2 chemicals proceeds through different reaction pathways as proposed previously.[13]

To study the effect of composition on catalyst activity and selectivity, we prepared two samples with different Cu:Pd ratios for the disordered structure: Cu3Pd (Cu_{at}:Pd_{at} = 3:1) and CuPd3 (Cu_{at}:Pd_{at} = 1:3). The HR-TEM data (Figure S4) show that the morphologies of Cu3Pd and CuPd3 resemble the disordered CuPd sample. The crystalline structure of Cu3Pd is similar to that of the disordered CuPd sample, with some shoulder peaks around 35°−40° indicating the existence of oxides, while the crystalline structure of CuPd3 resembles that of fcc-type Pd (Figure S5). Next, we performed electrochemical characterization: The FEs for various products using these two samples, as well as the disordered CuPd sample, Cu nanoparticles (Cu-1 data from prior work under the same condition[19]), and Pd nanoparticles, are provided in Figure 3. As the concentration of Cu increases from

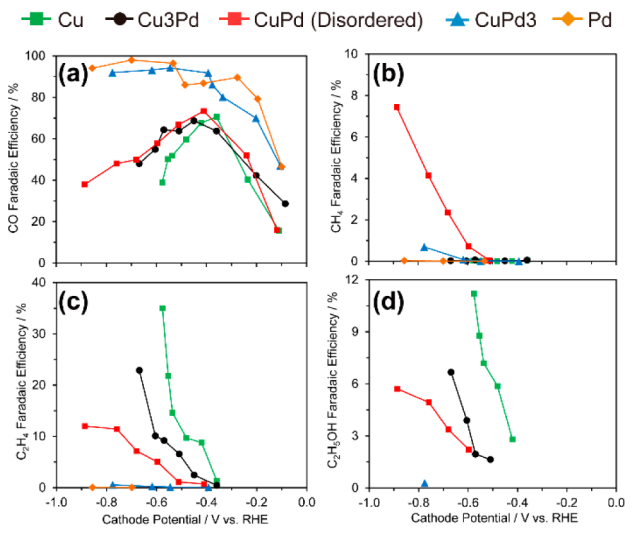

Figure 3. Faradaic efficiencies for (a) CO; (b) CH_4; (c) C_2H_4; (d) C_2H_5OH for catalysts with different Cu:Pd ratios: Cu, Cu3Pd, CuPd, CuPd3, and Pd.

Pd, CuPd3, CuPd to Cu3Pd and Cu, the FEs for C2 products increase. This observation further supports the idea that the dimerization of adsorbed CO to form C2 chemicals may be preferred on the sites with neighboring Cu atoms. The CH_4 FEs for both Cu3Pd and CuPd3 are lower than that for the disordered CuPd, probably due to the lower amount of Cu−Pd intermetallic sites within these two samples compared to the disordered CuPd. The disordered CuPd, Cu3Pd, and CuPd3 have different FEs for C2 chemicals despite their similar morphology. The fact that the phase-separated CuPd achieves the highest total current density despite its large particle size further indicates that the difference in morphologies and particle size among the samples probably is not the major cause for the observed differences in performance for the different catalyst structures shown in Figure 2.

We also suspect that electronic effects induced after mixing Cu with Pd may cause some of the observed differences in FEs for various products. To confirm this possibility, surface valence band photoemission spectra of the ordered, disordered, and phase-

DOI: 10.1021/jacs.6b10740
J. Am. Chem. Soc. 2017, 139, 47−50

separated samples, as well as Cu and Pd nanoparticles, were collected. The d-band centers of these samples relative to the Fermi level are plotted in Figure 4. According to Hammer and

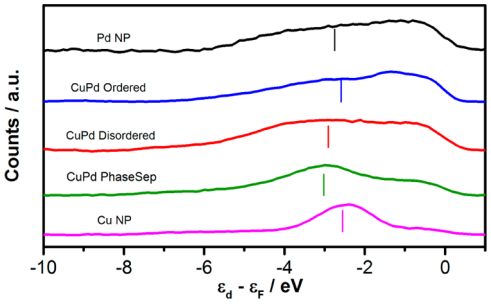

Figure 4. Surface valence band photoemission spectra of CuPd nanoalloys relative to Fermi level. All the spectra are background corrected. The vertical line indicates the d-band center of each sample relative to Fermi level.

Norskov,[21] for different transition metals, a lower d-band position (relative to the Fermi level) leads to weaker binding between the intermediate and the catalyst surface due to the occupancy of antibonding states. Phase separated CuPd has the lowest lying d-band center, while Cu nanoparticles have the highest lying d-band center (Figure 4), which indicates that the phase separated CuPd should have the weakest binding, while Cu nanoparticles should have the strongest binding with CO. However, since phase separated CuPd and Cu nanoparticles have similar catalytic selectivity and activity, geometric/structural effects probably play a more important role rather than electronic effects to determine catalytic selectivity and activity among various alloy samples in this study. Specifically, we suspect that the different mixing patterns of Cu and Pd atoms in various samples cause different orientations of the intermediate on the surface, therefore leading to different selectivities. In homogeneous catalysis, the orientation of intermediates toward the active site affects reaction activity.[22] Here, we suspect similar effects occur on the alloys with different mixing patterns.

In summary, through the synthesis and characterization of bimetallic Cu−Pd catalysts with different elemental mixing patterns and compositions, we demonstrate that mixing patterns of the components play an important role in determining each catalyst's activity and selectivity. The sample that features neighboring Cu atoms (phase-separated) favors production of C2 products, while the sample that features the alternating Cu−Pd arrangement favors the production of CH_4. This finding provides insight for the design of even better Cu-based alloy catalysts for the conversion of CO_2 to desired products. Maintaining the neighboring Cu sites while alloying with other transition metal atoms seems to be important. Computational studies on determining the actual number of Cu atoms within the active site for the production of C2 chemicals would be desired in the future.

■ ASSOCIATED CONTENT

Supporting Information

The Supporting Information is available free of charge on the ACS Publications website at DOI: 10.1021/jacs.6b10740.

Experimental details and data (PDF)

■ AUTHOR INFORMATION

Corresponding Authors

*yamauchi@i2cner.kyushu-u.ac.jp
*kenis@illinois.edu

ORCID

Richard T. Haasch: 0000-0001-9479-2595
Paul J. A. Kenis: 0000-0001-7348-0381

Present Address

⊥Opus 12, 2342 Shattuck Ave., Berkeley, CA 94704, USA.

Notes

The authors declare no competing financial interest.

■ ACKNOWLEDGMENTS

We gratefully acknowledge the support of the International Institute for Carbon Neutral Energy Research (WPI-I2CNER), sponsored by the Japanese Ministry of Education, Culture, Sports, Science and Technology. This work was also partially supported by JST-CREST and JSPS KAKENHI Grants 25288030, 24655040, 24850013, and 21350031. S.M. acknowledges support from FMC Educational Fund for a FMC Graduate Fellowship.

■ REFERENCES

(1) Pacala, S.; Socolow, R. *Science* **2004**, *305*, 968.
(2) Appel, A. M.; Bercaw, J. E.; Bocarsly, A. B.; Dobbek, H.; DuBois, D. L.; Dupuis, M.; Ferry, J. G.; Fujita, E.; Hille, R.; Kenis, P. J. A.; Kerfeld, C. A.; Morris, R. H.; Peden, C. H. F.; Portis, A. R.; Ragsdale, S. W.; Rauchfuss, T. B.; Reek, J. N. H.; Seefeldt, L. C.; Thauer, R. K.; Waldrop, G. L. *Chem. Rev.* **2013**, *113*, 6621.
(3) Jhong, H.-R. M.; Ma, S.; Kenis, P. J. A. *Curr. Opin. Chem. Eng.* **2013**, *2*, 191.
(4) Whipple, D. T.; Finke, E. C.; Kenis, P. J. A. *Electrochem. Solid-State Lett.* **2010**, *13*, B109.
(5) Hori, Y. In *Modern Aspects of Electrochemistry*; Vayenas, C., White, R., Gamboa-Aldeco, M., Eds.; Springer: New York, 2008; Vol. *42*, p 89.
(6) Kuhl, K. P.; Cave, E. R.; Abram, D. N.; Jaramillo, T. F. *Energy Environ. Sci.* **2012**, *5*, 7050.
(7) Roberts, F. S.; Kuhl, K. P.; Nilsson, A. *Angew. Chem.* **2015**, *127*, 5268.
(8) Li, C. W.; Kanan, M. W. *J. Am. Chem. Soc.* **2012**, *134*, 7231.
(9) Ren, D.; Deng, Y.; Handoko, A. D.; Chen, C. S.; Malkhandi, S.; Yeo, B. S. *ACS Catal.* **2015**, *5*, 2814.
(10) Kas, R.; Kortlever, R.; Milbrat, A.; Koper, M. T. M.; Mul, G.; Baltrusaitis, J. *Phys. Chem. Chem. Phys.* **2014**, *16*, 12194.
(11) Peterson, A. A.; Abild-Pedersen, F.; Studt, F.; Rossmeisl, J.; Norskov, J. K. *Energy Environ. Sci.* **2010**, *3*, 1311.
(12) Calle-Vallejo, F.; Koper, M. T. M. *Angew. Chem.* **2013**, *125*, 7423.
(13) Schouten, K. J. P.; Kwon, Y.; van der Ham, C. J. M.; Qin, Z.; Koper, M. T. M. *Chem. Sci.* **2011**, *2*, 1902.
(14) Peterson, A. A.; Nørskov, J. K. *J. Phys. Chem. Lett.* **2012**, *3*, 251.
(15) Kim, D.; Resasco, J.; Yu, Y.; Asiri, A. M.; Yang, P. *Nat. Commun.* **2014**, *5*.
(16) Zhang, S.; Kang, P.; Bakir, M.; Lapides, A. M.; Dares, C. J.; Meyer, T. J. *Proc. Natl. Acad. Sci. U. S. A.* **2015**, *112*, 15809.
(17) Monzo, J.; Malewski, Y.; Kortlever, R.; Vidal-Iglesias, F. J.; Solla-Gullon, J.; Koper, M. T. M.; Rodriguez, P. *J. Mater. Chem. A* **2015**, *3*, 23690.
(18) Yamauchi, M.; Tsukuda, T. *Dalton Trans.* **2011**, *40*, 4842.
(19) Ma, S.; Sadakiyo, M.; Luo, R.; Heima, M.; Yamauchi, M.; Kenis, P. J. A. *J. Power Sources* **2016**, *301*, 219.
(20) Li, C. W.; Ciston, J.; Kanan, M. W. *Nature* **2014**, *508*, 504.
(21) Hammer, B.; Nørskov, J. K. *Advances in Catalysis*; Academic Press: 2000; Vol. *45*, p 71.
(22) Straub, B. F. *Angew. Chem., Int. Ed.* **2005**, *44*, 5974.

DOI: 10.1021/jacs.6b10740
J. Am. Chem. Soc. 2017, 139, 47−50